EPJ Web of Conferences **266**, 13024 (2022)
EOSAM 2022
https://doi.org/10.1051/epjconf/202226613024

Experimental evaluation of Fourier transform holograms by a self-interferometric technique

Esther Nabadda[1], *Pascuala* Garcia-Martínez[2], *María de Mar* Sánchez-López[1,3] and *Ignacio* Moreno[1,4*]

[1]Instituto de Bioingeniería, Universidad Miguel Hernández de Elche, 03202 Elche, Spain
[2]Departamento de Óptica y Optometría y Ciencias de la Visión, Universitat de València, 46100 Burjassot, Spain
[3]Departamento de Física Aplicada, Universidad Miguel Hernández de Elche, 03202 Elche, Spain
[4]Departamento de Ciencia de Materiales, Óptica y Tecnología Electrónica, Universidad Miguel Hernández de Elche, 03202 Elche, Spain

Abstract. We present a technique that combines an encoding method to display complex-valued holograms onto a phase-only spatial light modulator (SLM) with a phase-shifting interferometric (PSI) technique for experimentally evaluating the generated complex-valued optical fields. We demonstrate an efficient common-path polarization interferometer based on the SLM itself, not requiring any external additional element. The same setup can be used to simultaneously display the complex hologram and to apply the phase-shifting values required to retrieve the phase distribution of the optical field. A simple rotation of a polarizer allows to change from the intensity configuration to the interferometer configuration.

1 Introduction

Parallel-aligned liquid-crystal on silicon (LCOS) displays are pixelated linear retarders that, under illumination with linearly polarized light parallel to the liquid-crystal (LC) director, produce a phase-only modulation [1]. They have become very popular spatial light modulator (SLM) devices for diffractive optics and structured light.

On the other hand, liquid crystal retarders are very useful devices in interferometry. In phase-shifting interferometry (PSI) they are employed to impart controlled phase bias to the interferograms to retrieve the target phase function [2]. LC-SLMs can be used to display spatially retardance functions that provide a common-path interferometric arrangement [3].

In this communication we present an extremely simple technique that makes the most of these properties to retrieve the complex information of light beams generated with an LCOS-SLM. We first apply a technique to encode complex-valued holograms based on displaying a modified checkerboard grating, useful to provide an on-axis hologram reconstruction [4-6]. The technique is demonstrated by producing different superpositions of Gaussian modes. The successful generation of these structured light beams is verified by capturing the intensity pattern in the far field. Then, the same optical system employed to generate the structured light beams is also applied to retrieve the far field phase distribution through a PSI algorithm. The change in the optical setup consists simply in rotating a polarizer. The application of PSI algorithms provides quantitative evaluation of the phase distribution that complements the traditional intensity pattern evaluation

2 Methods and techniques

2.1 Experimental setup

Figure 1 shows the experimental arrangement. A linearly polarized He-Ne laser is spatially filtered and collimated. A quarter-wave plate (QWP) converts it into circularly polarized light, so a linear polarizer (P1) can rotate arbitrarily without changing the light intensity. The beam illuminates an LCOS-SLM (Hamamatsu X10468-01, with 800×600 pixels of 20 μm pitch). The LCOS-SLM has its director axis oriented horizontally with respect to the laboratory framework and is addressed with a hologram that includes the phase of a converging lens. A camera is placed on its back focal plane, thus capturing the Fourier transform pattern generated by the hologram.

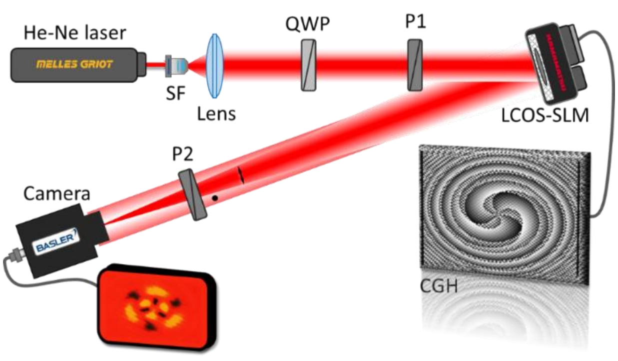

Fig. 1. Scheme of the optical system. SF: spatial filter; QWP: quarter-wave plate; P: linear polarizer; LCOS-SLM: Liquid-crystal on silicon spatial light modulator; CGH: displayed phase-only computer-generated hologram.

* Corresponding author: i.moreno@umh.es

2.2 Hologram design

A complex function $F(\mathbf{r}) = M(\mathbf{r})\exp[i\theta(\mathbf{r})]$ must be encoded on the SLM. Here $\mathbf{r} = (x, y)$ are the spatial coordinates. Since the LCOS device is a phase-only modulator, a new phase-only hologram is calculated as the following phase function

$$\phi_H(\mathbf{r}) = \theta(\mathbf{r}) + (-1)^{m+n}\arccos[M(\mathbf{r})]. \qquad (1)$$

A converging lens phase function $\phi_L(\boldsymbol{r}) = -\pi r^2/\lambda f$ is added, where $r = |\mathbf{r}|$ is the radial coordinate, λ is the operating wavelength and f is the lens focal length. The phase function $\phi(\boldsymbol{r}) = \phi_H(\boldsymbol{r}) + \phi_L(\boldsymbol{r}) + \varphi_n$ is then displayed on the SLM. The phase φ_n is a constant phase bias, which does not change the spatial pattern generated in the far field, but is used to apply the PSI algorithm.

2.3. Interferometer configuration

If polarizer P1 in Fig. 1 is aligned parallel to the SLM LC director, all the light is modulated and focused on the camera, which captures the intensity of the hologram reconstruction. However, if P1 rotates to another angle, a portion of the input light is not modulated and remains collimated and can be used as the reference beam. Polarizer P2 is oriented at 45º so the components parallel and perpendicular to the LC director interfere, in a common path arrangement. The relative intensity of the reference and the test beams can be adjusted by rotating P1, while the PSI algorithms can be applied by changing the bias phase φ_n. Note that an arbitrary number of phase shifts can be applied, so different PSI algorithms can be tested. In our case we chose a synchronous detection algorithm with eight steps shifted by $\pi/4$ radians, leading to the following phase retrieving formula [7]:

$$\alpha(\boldsymbol{r}) = -\arctan\left\{\frac{2(I_0-I_4)+\sqrt{2}(I_1-I_3-I_5+I_7)}{2(I_2-I_6)+\sqrt{2}(I_1+I_3-I_5-I_7)}\right\}. \qquad (2)$$

3 Results

Figure 2 shows some experiments where a Hermite-Gauss HG_{33} beam and a Laguerre-Gauss LG_{13} beam are encoded. Figures 2(a)-2(b) and 2(e)-2(f) show their theoretical intensity and phase patterns. Figures 2(c) and 2(g) show the experimental intensity distributions captured on the camera, while Figs. 2(d) and 2(h) show the phase patterns $\alpha(\mathbf{r})$ retrieved from the eight interferograms, which are shown in the two rows below each case. Results bear very good agreement with the theory, thus confirming the successful generation of the HG and LG beams, not only in its intensity but also in its phase distribution, which probes the accuracy and advantage of this technique. Other cases obtained by the superposition of different modes have been succesfully generated and will be presented.

Acknowledgements: This work received financial support from Ministerio de Ciencia, Innovación y Universidades, Spain (grant RTI2018-097107-B-C33). E.N. acknowledges a grant from Generalitat Valenciana, Santiago Grisolia Program (ref. GRISOLIAP/2020/004).

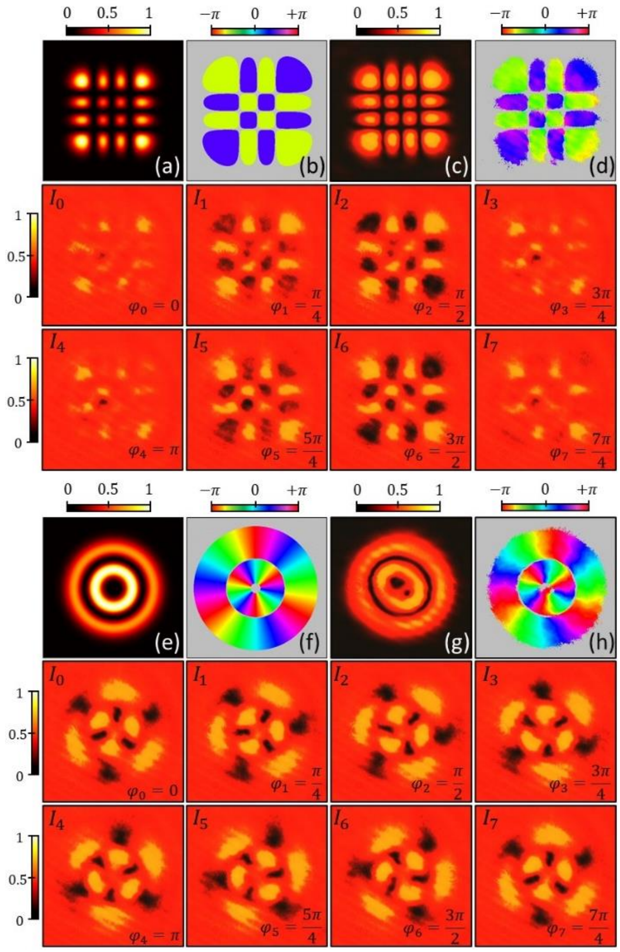

Fig. 2. Realization of a HG_{33} (a-d) and LG_{13} (e-h) beam. Theoretical intensity (a,e) and phase (b,f) distributions. Experimental intensity (c,g) and phase (d,h) distributions. The phase distribution of each beam is retrieved from the interferograms shown below each case with eight consecutive phase shifts of step $\Delta\varphi = \pi/4$.

References

1. Z. Zhang, Z. You, D. Chu, Light: Sci. Appl. **3**, 213 (2014).
2. Y.B. Machuca-Bautista, M. Strojnik, J.L. Flores, D.I. Serrano-García, G. García-Torales, Results Opt. **5**, 100197 (2021).
3. I. Moreno, J.A. Davis, F.A. Klein, M.J. Mitry, Appl. Opt. **47**(11), 1797-1801 (2008).
4. V. Arrizón, Opt. Lett. **28**(24), 2521-2523 (2003).
5. O. Mendoza-Yero, G. Mínguez-Vega, J. Lancis, Opt. Lett. **39**(7), 1740-1743 (2014).
6. J.A. Davis, E.D. Wolfe, I. Moreno, D.M. Cottrell, OSA Continuum **4**(3), 896-910 (2021).
7. K. Creath, Prog. Optics **26**, 349-393 (1988).